Eur. Phys. J. D (2017) 71: 241
DOI: 10.1140/epjd/e2017-80073-2

THE EUROPEAN PHYSICAL JOURNAL D

Regular Article

γH2AX/53BP1 foci as a potential pre-treatment marker of HNSCC tumors radiosensitivity – preliminary methodological study and discussion*

Martin Falk[1,a], Zuzana Horakova[2], Marketa Svobodova[3,4], Michal Masarik[3,4], Olga Kopecna[1], Jaromir Gumulec[3,4], Martina Raudenska[3,4], Daniel Depes[1], Alena Bacikova[1], Iva Falkova[1], and Hana Binkova[2]

[1] Department of Cell Biology and Radiobiology, Institute of Biophysics of CAS, 61265 Brno, Czech Republic
[2] Department of Otorhinolaryngology and Head and Neck Surgery, St. Anne's University Hospital and Faculty of Medicine, Masaryk University, 65691 Brno, Czech Republic
[3] Department of Pathological Physiology, Faculty of Medicine, Masaryk University, 62500 Brno, Czech Republic
[4] Department of Physiology, Faculty of Medicine, Masaryk University, 62500 Brno, Czech Republic

Received 31 January 2017 / Received in final form 10 July 2017
Published online 19 September 2017 –

Abstract. In order to improve patients' post-treatment quality of life, a shift from surgery to non-surgical (chemo)radio-treatment is recognized in head and neck oncology. However, about half of HNSCC tumors are resistant to irradiation and an efficient marker of individual tumor radiosensitivity is still missing. We analyzed whether various parameters of DNA double strand break (DSB) repair determined in vitro can predict, prior to clinical treatment initiation, the radiosensitivity of tumors. We compared formation and decrease of γH2AX/53BP1 foci in 48 h after irradiating tumor cell primocultures with 2 Gy of γ-rays. To better understand complex tumor behavior, three different cell type primocultures – $CD90^-$, $CD90^+$, and a mixed culture of these cells – were isolated from 1 clinically radioresistant, 2 radiosensitive, and 4 undetermined HPV–HNSCC tumors and followed separately. While DSB repair was delayed and the number of persisting DSBs increased in the radiosensitive tumors, the results for the radioresistant tumor were similar to cultured normal human skin fibroblasts. Hence, DSB repair kinetics/efficiency may correlate with clinical response to radiotherapy for a subset of HNSCC tumors but the size (and therefore practical relevance) of this subset remains to be determined. The same is true for contribution of different cell type primocultures to tumor radioresistance.

1 Introduction

Head and neck squamous cell cancer (HNSCC; shortened here as HN) are usually aggressive neoplasms with high recurrence rate and poor prognosis. Due to their proximity to vital structures, efficient radical surgery results in patients' mutilation with impaired quality of life. Non-surgical (chemo-radiotherapy) approaches are therefore preferred but bear the risk of radioresistance resulting in the tumor persistence or even progression after treatment, which cannot always be salvaged by surgery. Indeed, about 52% of HN tumors resist to irradiation and results of the salvage surgery are in principle incomparable to those of primary surgery, with protracted healing and risk of unrecognizable tumor growth in the irradiated terrain [1,2]. Oncologists thus permanently face to a serious dilemma of the optimal first-line therapy for a particular patient (reviewed in [3]).

Unfortunately, the radioresistance markers allowing tumor radiosensitivity estimation prior to therapy are still unknown. Their discovery is largely complicated by genetic and functional heterogeneity of tumors that seems to be particularly high in HN. Unlike some other cancer types, HN tumors can be considered neither radiosensitive nor radioresistant, since these tumors occupy both extremes of the radiosensitivity spectrum (reviewed e.g. in [4]). Though some genes have been repeatedly found to be mutated in HN, there are not common 'founder' mutations associated with these malignancies ([5] and citations therein) and their radiosensitivity.

The radiosensitivity/radioresistance markers might be logically associated with complex cell response to DNA damage. Most relevant in this sense is probably repair of DNA double strand breaks (DSBs) since DSBs represent the most serious lesions being extensively introduced into the DNA molecule by ionizing radiation and some kinds of chemotherapy [6]. However, also genetic or epigenetic defects affecting other processes [7–16] such as resistance to apoptosis [7], defects in cell cycle regulation [8], ability

* Contribution to the Topical Issue "Dynamics of Systems at the Nanoscale", edited by Andrey Solov'yov and Andrei Korol.

[a] e-mail: falk@ibp.cz

to divide with damaged genome [9] or competency to re-enter cell cycling from senescence [10] (reviewed in [11,12]) can significantly contribute to final cell radioresistance. Eventually, those mechanisms might even play a major role.

Hence, it would not be surprising to discover that the basis of radioresistance differs among individual tumors. This expectation then almost precludes usage of model systems, such as permanent cell lines or transgenic mice, to study HN tumor biology and behavior. Moreover, even single tumors are highly heterogeneous and dynamic systems. Still undetermined source of radioresistance heterogeneity thus also comes from characteristics and proportion of different cell types, their specific clones, and mutual interactions among all these cells [17–19].

In this study, by using immunofluorescence confocal microscopy for sensitively quantifying γH2AX/53BP1 foci formation and decrease in post-irradiation (PI) time, we attempt to find out how individual HN tumors vary in DNA double-strand break (DSB) repair kinetics and efficiency, whether these characteristics correlate with tumor cells' radiosensitivity, and whether in vitro monitoring of DSB repair could be predictive of tumors' clinical response to radiotherapy. To address these questions and in a need to deeper explore biological determinants of HN tumors' radioresistance, we prepared from patients' tumors three different cell primocultures – the primoculture of epithelial tumor cells characterized by absence of CD90 surface antigen ($CD90^-$ cells), the primoculture of remaining cells that were CD90 positive ($CD90^+$ cells), and a mixed culture of both these cell types. CD90 cluster of definition is expressed in several cell types, including a fraction of fibroblasts; $CD90^+$ cells used in our experiments thus contain a significant fraction of tumor-associated fibroblasts (TAFs) that are, in addition to $CD90^-$ tumor cells, expected to influence tumors' biology and characteristics [17–19]. We describe here our first results comparing DSB repair between tumors for each specific cell primoculture and between the primocultures for each particular tumor.

2 Methods

2.1 HN tumor biopsy extraction

HN tumor biopsy extraction was performed in the Department of Otorhinolaryngology and Head and Neck Surgery, St. Anne's University Hospital and Faculty of Medicine, Masaryk University, Brno, Czech Republic. Patients were completely examined clinically and the tumor staging was determined using radiodiagnostic approaches (CT, MRI, PET). Only newly diagnosed patients with none previous therapeutic history and with HN squamous-cell carcinoma (HNSCC) confirmed histopathologically were included in the study, after signing the informed consent. Biopsy cell samples were obtained by endoscopy under local or total anesthesia.

2.2 Tumor cells primocultures

Tumor cells primocultures were prepared in the Department of Pathological Physiology, Faculty of Medicine, Masaryk University, Brno, Czech Republic. The tumor tissue material obtained at surgery (see Sect. 2.1) was placed into culture medium (RPMI 1640, Biochrom, USA) with an addition of 1% antibiotic-antimycotic solution (Santa Cruz Biotechnology, Texas), 10 $\mu g\,ml^{-1}$ gentamicin sulphate (Santa Cruz Biotechnology, Texas) and 10 $\mu g\,ml^{-1}$ ciprofloxacin (Santa Cruz Biotechnology, Texas) to prevent bacteria, fungi and yeast contamination. Within sterile environment and after rinsing the sample by 70% EtOH (Sigma-Aldrich, Germany), the most viable tissue was selected while any necrotic tissue was discarded. Leavings of EtOH were removed by PBS (Invitrogen, USA) washing. Tissue was mechanically dissociated into small pieces and Trypsin (PAA Laboratories GmbH, Austria for proteolysis were used) was used according to Protocol 1 (below) to separate the cells.

Protocol 1. The small tissue fragments were added and stirred into sterile PBS (Invitrogen, USA) and centrifuged at 4 °C, 2700 rpm for 7 min. The cell pellet was re-suspended into 0.25% trypsin in RPMI 1640 medium and left overnight at 4 °C. Then medium was removed and tissue was incubated at 37 °C for 30 min. The cell pellet was re-suspended into medium with an addition of antibiotic-antimycotic solution, gentamicin sulphate, ciprofloxacin and 10% FBS. Primary cell lines were cultivated at 37 °C and 5% CO_2 in humidified atmosphere up to 50% confluence. As soon as the cells were seen attaching to the flask surface, medium was changed. Tumor cells were no longer affected by the use of antibiotic-antimycotic solution, gentamicin sulphate, or ciprofloxacin that were added to the early culture. At this time, cells were grown only in Pen/Strep antibiotic solution (PAA Laboratories GmbH, Austria) in the complete medium (penicillin 100 U ml^{-1} and streptomycin 0.1 mg ml^{-1}; RPMI-1640 medium with 10% FBS (Biochrom, USA)).

For separation of subpopulation derived from primary cell line magnetic particles-MiniMACS^{TM} Starting Kit (CD90 MicroBeads-human, MS Columns; Miltenyi Biotec, Germany) was used. Cells that adhered to the flask were grown in complete medium (RPMI-1640 medium with 10% FBS, penicillin 100 U ml^{-1} and streptomycin 0.1 mg ml^{-1}) until they reach 70% confluency; they were then passaged. For each tumor, we prepared separated primocultures for $CD90^-$, $CD90^+$, and their mixed co-culture serving to study possible interactions between the cell types. The whole procedure is described in Svobodova et al. (2017) (Oncotarget; DOI:10.18632/oncotarget.19914).

2.3 Irradiation with γ-rays

The cells were irradiated at the Institute of Biophysics, Czech Academy of Sciences, Brno, Czech Republic. In our first experiments, presented here, we irradiated the cell lines with a single dose of 2 Gy ($D = 1$ Gy/min) of γ-rays

Table 1. Tumors characteristics.

Patient	Sex	Age [y]	Tumor	Locality	Stage	Grade	Therapy	RT response	Current status, other characteristics
T1	m	60	SCC	OP	IV T4 N2b	G3	RT + BT	S	UT BT: cetuximab
T2	m	70	SCC	HL	T3 N1	G3	S + RT	S	REM (6 month) total laryngectomy + adjuv. RT
T3	m	66	SCC	L	II T2N0	G2	RT	R	UT tripl CA (mammary + renal + HN)
T4	m	77	SCC	OP	IV T4b N3	G2	None	?	†
T5	m	70	SCC	LHP	IV T3N1	G3	S + RT	?	REM (4 month) total laryngectomy + adjuv. RT
T6	f	90	SCC	OHP	IV T4N2	G3	None	?	†
T7	m							?	

Legend: m: male, f: female, OP: oropharynx, L: Larynx, HL: hypolarynx, LHP: laryngohypopharynx, OHP: orohypopharynx, RT: radiotherapy, S: surgery, BT: biological treatment, R: radioresistant (none/poor response), S: radiosensitive (good response), †: died, UT: under treatment, REM: remission.

(^{60}Co, Chisostat, Chirana, CR). Cells were irradiated in RPMI 1640 medium (37 °C, normal atmosphere) [20].

2.4 Evaluation of DNA double strand break (DSB) induction and repair in tumor cell primocultures

The evaluation of DSB induction and repair was performed at the Institute of Biophysics, Czech Academy of Sciences, Brno, Czech Republic. DSBs were quantified in different periods of time post-irradiation (5 min–48 h PI) by means of γH2AX and 53BP1 foci immunodetection combined with high-resolution 3D confocal microscopy. For more detailed description of visualization of γH2AX and 53BP1 in spatially (3D) fixed cells see [21].

2.5 3D high-resolution confocal microscopy

The microscopy of samples was performed at the Institute of Biophysics, Czech Academy of Sciences, Brno, Czech Republic. Leica DM RXA microscope [22] (equipped with DMSTC motorized stage, Piezzo z-movement, MicroMax CCD camera, CSU-10 confocal unit and 488, 562, and 714 nm laser diodes with AOTF) was used for acquiring detailed cell images (100× oil immersion Plan Fluotar lens, NA 1.3). The equipment was controlled by the Acquarium software developed in collaboration with Masaryk University [23]. Modern Leica SP5 microscopy system, equipped with white laser for multicolor microscopy, allowed "high-throughput" cell imaging [21]. Images were reconstructed and analysed in Acquarium (FI MU, Brno), LAS AF (Leica), Adobe Photoshop CS5 (Adobe), and ImageJ software. DSB repair foci were scored also manually by two experienced examiners. Though absolute numbers of foci were lower for software analyses, the trends for manual and software scoring were the same. SigmaPlot Scientific Software (SPSS, Systat Software, Inc.) was used for statistical evaluation of data.

3 Results

3.1 Patients/tumors characteristics

HNSCC tumor biopsies were taken from 5 patients' primary tumors after confirming SCC by conventional histopathology and signing the informed consent. Patients were completely examined clinically and basic tumor characteristics were determined (Tab. 1). Radiodiagnostic approaches (CT, MRI, PET) were employed to determine tumors' staging. Only patients with newly diagnosed HPV–HNSCC with none therapeutic history and recommended for non surgical treatment were included into the study; the purpose for this decision was to minimize unwanted biological/experimental variability and allow later comparison of results obtained in vitro to histopathological characteristics of tumors and their response to radiotherapy in vivo. From 7 tumors currently included into the study, 1 tumor (T3) was radioresistant, 2 tumors (T1 and T2) were radiosensitive, and the status of remaining tumors was unsure (patients died without treatment, etc.).

Regarding oncologic prognosis and quality of life, our collected therapeutic results from last 15 years show that the optimal treatment strategy for an individual patient can be still determined only with difficulty and low fidelity if it is only based on clinical data and/or tumors' response to chemotherapy [1,2]. Identification of marker(s) allowing radiosensitivity estimation prior to the therapy initiation therefore still remains of utmost importance.

3.2 Methodological strategy and results

3.2.1 Preparation and characterization of CD90$^-$ and CD90$^+$ cell primocultures

In order to deeper comprehend the phenomenon of tumor radiosensitivity, we decided to compare DSB repair

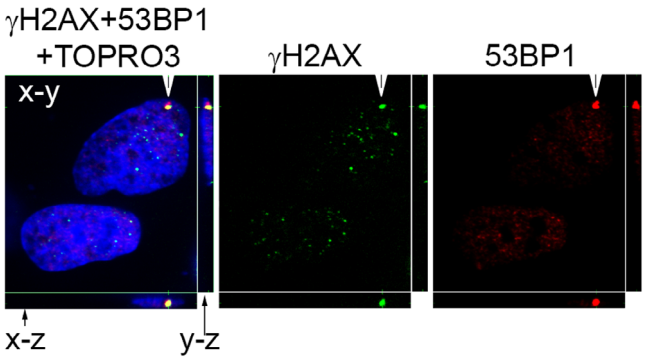

Fig. 1. Sensitive detection of DSBs by means of immunofluorescence confocal microscopy. Two DSB markers – γH2AX (green) and 53BP1 (red) – are detected simultaneously in spatially (3D) fixed cells. A single DSB detected in one of displayed non-irradiated human normal skin fibroblasts (top one) is indicated by colocalizing green and red signals (white arrow). This approach currently brings the maximum sensitivity and precision in DSB quantification. A single confocal slice (0.3 μm thick) through the cell nuclei in the plane of detected DSB is shown. Chromatin counterstaining by TOPRO3 (artificially blue); magnification 100×.

for two important cell types inhabiting the tumors – CD90$^-$ and CD90$^+$ cells – and for their mixed culture (CD90$^-$ + CD90$^+$). For this purpose, we developed and optimized [24] a protocol for immunoseparation of CD90$^-$ and CD90$^+$ from tumors according to their CD90 cluster of definition (surface CD antigens [25]). Using the procedure described in Section 2, the two cell types were successfully separated and their primocultures prepared and basically characterized in terms of gene expression. Interestingly, expression of some important genes, such as EGFR, MMP2 and MT2 in CD90$^+$ cells isolated from tumors resembled more tumor CD90$^-$ cells than normal CD90$^+$ fibroblasts (not shown).

3.2.2 Introduction of immunofluorescence confocal microscopy for DSB repair monitoring in CD90$^-$ and CD90$^+$ cell primocultures

Immunofluorescence confocal microscopy of γH2AX foci currently represents the most sensitive method to quantify DSBs [26]. This is demonstrated also by present results (Fig. 1) successfully revealing even occasional DSBs occurring in non-irradiated nonmalignant human skin fibroblasts (NHDF cells). Therefore, in this work, we tested applicability of γH2AX foci immunodetection as a tool to predict tumors' radiosensitivity/radioresistance in vitro and to study complex response of tumor cells to irradiation. To further maximize sensitivity and fidelity of the method, we decided to analyze two independent DSB markers – γH2AX and 53BP1 foci – in spatially (3D) fixed cells simultaneously (Fig. 1) [20,27]. Successful application of γH2AX/53BP1 foci immunofluorescence confocal microscopy to monitor DSB repair kinetics and efficiency in tumor cell primocultures is illustrated in Figure 2.

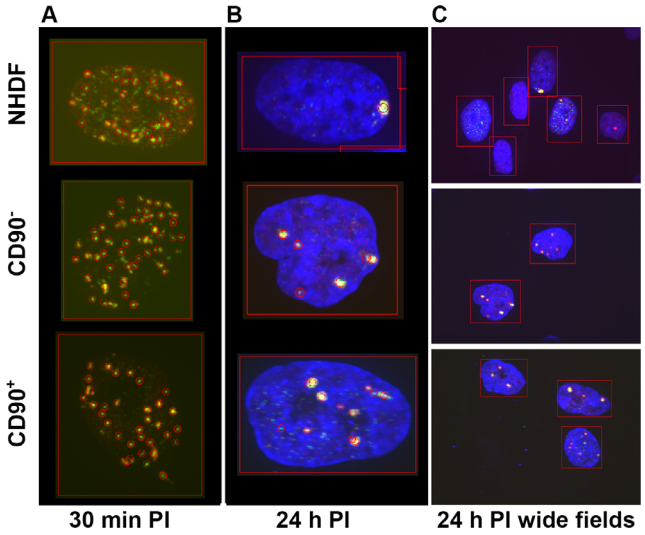

Fig. 2. γH2AX (green) and 53BP1 (red) repair foci co-detected by immunofluorescence confocal microscopy in irradiated (2 Gy of γ-rays; D = 1 Gy/min) normal human skin fibroblasts (NHDF) and CD90$^-$ and CD90$^+$ cell primocultures obtained from the radioresistant tumor T3 (see Tab. 1 for the tumor characteristics). The cells were spatially (3D) fixed and immunoassayed at 30 min (A) and 24 h (B, C) post-irradiation, respectively. Panel C shows wide-field images with more cells. Maximum images composed of 30 confocal slices 0.3 μm wide are shown. In B and C, chromatin is counterstained with TOPRO3 (artificially blue) while this staining is absent in A in order to make γH2AX (green) + 53BP1 (red) foci better visible. Foci detected by automatic software analyses are indicated by red circles (A, B, C). Magnification 100×.

3.3 DSB repair in CD90$^-$ and CD90$^+$ cell primocultures

Figure 2 shows illustrative microscopy images for normal human skin fibroblasts (NHDF) and CD90$^-$ and CD90$^+$ cells isolated from the radioresistant tumor T3 (see Tab. 1 for characteristics); mutually colocalizing γH2AX and 53BP1 foci were immunodetected at 30 min and 24 h after irradiation of the cells with 2 Gy (1 Gy/min) of γ-rays. While formation of γH2AX/53BP1 foci at 30 min PI (maximum DSB induction) was similar for all three cell types, an increased presence of foci at 24 h PI (persistence of unrepaired DSBs), relative to normal NHDF, could be seen in CD90$^-$ and CD90$^+$ radioresistant tumor primocultures. Figure 3 then provides detailed quantitative comparisons on DSB repair kinetics and efficiency for normal cultured fibroblasts and the mixed CD90$^-$ + CD90$^+$ primocultures isolated from radiosensitive (T1 and T2) and radioresistant (T3) tumors, respectively. Data for tumors T4–T7 are not displayed for their unknown clinical radiosensitivity and to allow better readability of the graphs. For all tumors, irrespective of their radiosensitivity status, the maximum DSB induction appeared at 30 min PI; however, the kinetics of γH2AX/53BP1 foci disappearance varied with samples: While DSB repair kinetics for the radioresistant tumor T3 closely resembled that of normal cultured fibroblasts, a significant delay of this process

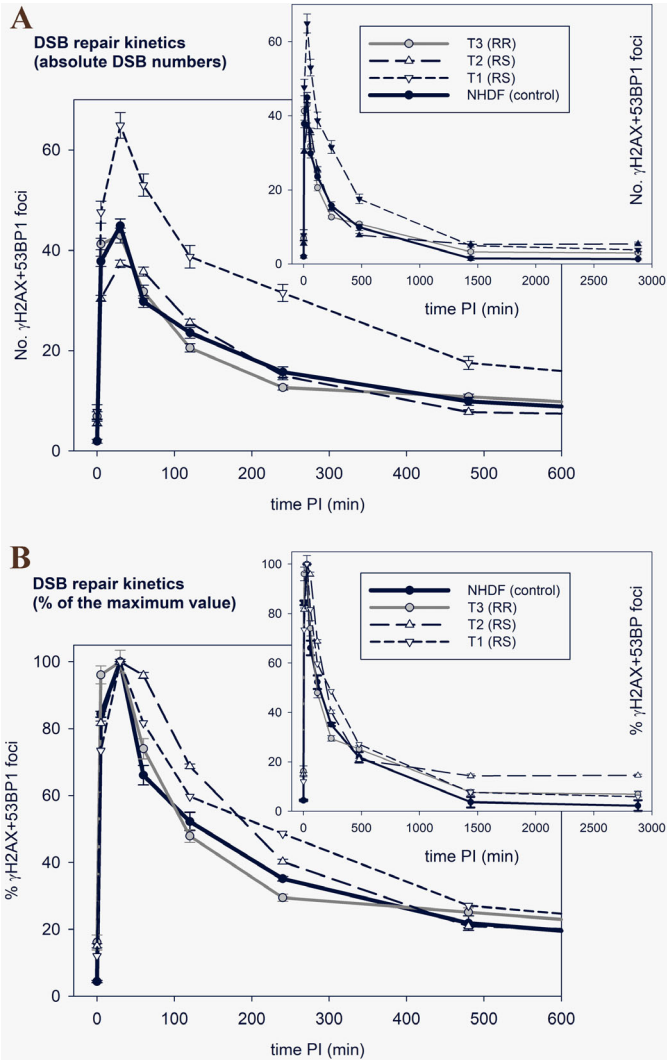

Fig. 3. γH2AX/53BP1 foci formation, disappearance and persistence (DSB repair kinetics and efficiency) compared for normal human skin fibroblasts (NHDF) and CD90$^+$ tumor cells primocultures derived from clinically radiosensitive (T1 and T2) and radioresistant (T3) tumors, respectively. See Table 1 for the tumors' characteristics. A: The mean numbers of γH2AX/53BP1 foci per nucleus during the time post-irradiation with 2 Gy of γ-rays. The values obtained by immunofluorescence confocal microscopy in spatially (3D) fixed cells are shown. Error bars represent standard deviations (T1, T2 and T3) or standard errors of means (NHDF) calculated for two independent experiments. B: As A but the percentage of γH2AX/53BP1 foci per nucleus is shown (100% correspond to the maximum value detected for all samples at 30 min PI).

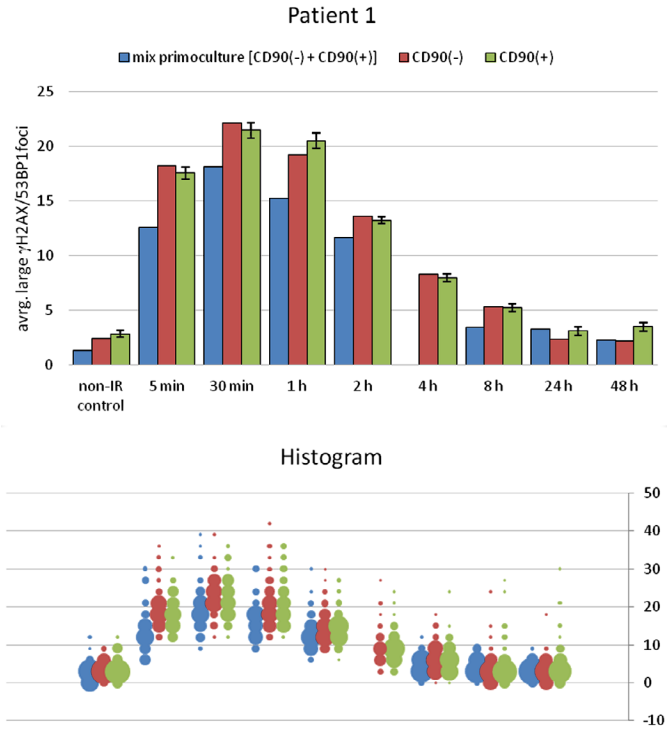

Fig. 4. DSB induction and repair compared for CD90$^-$ and CD90$^+$ cells and for their mixed culture (CD90$^-$ + CD90$^+$); all primocultures were derived from the radiosensitive tumor T1. Mean values of large γH2AX/53BP1 foci per nucleus are shown with standard errors.

appeared in the case of both radiosensitive tumors, T1 and T2 (Fig. 3). Nevertheless, the reason for this repair delay differed: In T1, the average number of DSBs per nucleus induced by 2 Gy of γ-rays dramatically exceeded that in NHDF fibroblasts and also all other tumors. This situation followed from an enormous size of T1 cells and extremely slowed the removal of DSBs (Fig. 3A), though the repair efficiency seemed to be unaffected (Fig. 3B). In contrast, both the average maximum number of γH2AX/53BP1 foci per nucleus and DSB repair efficiency were low in tumor T2 (Figs. 3A and 3B).

Moreover, the amount of γH2AX/53BP1 foci detected in non-irradiated cells (genomic instability) and the amount of foci persisting in cells long periods of time post-irradiation (48 h PI; DSB repair inefficiency/DSB tolerance) were increased (as compared to NHDF) in all tumors but especially in both radiosensitive tumors (Fig. 3). For the radiosensitive tumors T1 and T2 the numbers of persisting foci exceeded the average value measured for NHDF significantly (Fig. 3).

Experiments with separated CD90$^-$ and CD90$^+$ cell primocultures provided the results that were mutually comparable and roughly resembled those described above for the mixed CD90$^-$ + CD90$^+$ cultures; however, in several cases, the mixed CD90$^-$ + CD90$^+$ cultures showed lower formation and faster disappearance of γH2AX/53BP1 foci than we observed for both CD90$^-$ and CD90$^+$ cells. The results for tumor T1 are provided as an example in Figure 4.

4 Discussion

While only about 50% of HN tumors respond to irradiation [1,2], radiotherapy is being applied more or less "randomly" since any effective and reliable method to identify radiosensitive tumors has not been implemented yet. HN tumors to be treated by radiotherapy are therefore

only selected on the basis of their clinical parameters and/or response to neoadjuvant chemotherapy. However, our clinical experience from past 15 years (180–220 newly diagnosed patients/year) shows that the chemosensitivity of HN tumors (with the highest share of laryngeal, oropharyngeal and hypofaryngeal locality, mostly in advanced stage) does not sufficiently correlate with the radiosensitivity. Searching for a more direct and reliable HN tumor radiosensitivity/radioresistance marker thus still represents an important task of radiobiological research.

Though many other processes may also contribute, the repair of DSBs could be suspected of substantially determining the tumors' radiosensitivity/resistance. This is because DSBs represent the most lethal DNA damage being introduced into DNA of affected cells by radiotherapy and some kinds of chemotherapy. In this work, therefore, we tested this hypothesis for HN tumors and analyzed the possibility whether evaluation of DSB repair in tumor cell primocultures irradiated in vitro might open new way to predict an individual-specific response to radiotherapy [28].

We succeeded with introducing methods for preparing separate primocultures of different cell types from HN tumors and employed currently the most sensitive method – immunofluorescence confocal microscopy of γH2AX/53BP1 repair foci [27] – to monitor DSB induction and repair in these primocultures prior to and upon irradiation. We have demonstrated already earlier that results of γH2AX/53BP1 immunofluorescence microscopy well correlate with comet assay, the gold standard method in radiobiology to directly quantify DSBs [27]. Taking advantage of the described approach, we compared various parameters of DSB repair for $CD90^-$, $CD90^+$ and $CD90^-$ + $CD90^+$ tumor cell primocultures derived from 7 HN tumors, where 1 tumor was clinically radioresistant, 2 tumors were radiosensitive and remaining tumors were of unknown status. The reason for separating cells according to the CD90 surface antigen positivity is as follows: though there are some uncertainties in the literature about interpretation of CD90 expression, we can reasonably suppose that $CD90^-$ cells in our study represent epithelial tumor cells while $CD90^+$ cells contain a predominant fraction of tumor-associated fibroblasts (TAFs). Important roles of TAFs in influencing malignant potential and treatment response of tumors have repeatedly been described (e.g. [29] and citations therein). The mixed $CD90^-$+$CD90^+$ primoculture allowed us to reveal potential influence of $CD90^-$ and $CD90^+$ cell interactions on DSB repair.

Cultured human skin fibroblast (NHDF) provided us DSB repair characteristics for normal, non-malignant cells and served thus as the patient-independent DSB repair standard. Comparisons of results to normal mucosa cells extracted from histologically normal HN tissues (e.g. tonsils) of corresponding HN cancer patients were impossible for present tumors; however, we hope to obtain such data at least for some tumors in future. This information will allow for determining the patient-specific DSB repair efficiency-ratio between normal and tumor cells, while comparison with NHDF cell line may reveal potential functional (DSB repair) or even pre-malignant alterations in histologically normal patients' tissues far distant from the tumor [30,31]. The results may contribute to our better understanding of tumor development as well as to better therapy planning in future.

We first analyzed presence of DSBs in non-irradiated NHDF cells and tumor primocultures (see Fig. 3). The results revealed that even non-irradiated $CD90^-$, $CD90^+$, and $CD90^-$ + $CD90^+$ primocultures derived from the radioresistant tumor T3 show markedly higher average numbers of γH2AX/53BP1 foci per nucleus than NHDF cells. Since increased numbers of γH2AX/53BP1 repair foci appeared in the majority of cells, we suppose this observation reveals increased genomic instability in all three tumor T3 primocultures, rather than their higher mitotic activity. Though, both these possibilities might be not mutually exclusive and further experiments are necessary to shed more light on this phenomenon. Interestingly, non-irradiated primocultures isolated from radiosensitive tumors T1 and T2 also obtained increased foci numbers, higher than NHDF cells. Hence, more tumors must be analyzed to find out whether the genomic instability may point more generally to a higher tumor radioresistance. One explanation could consist in the fact that tumors with a higher level of genetic heterogeneity contain increased frequencies of cell clones, where some of them might exhibit radioresistant features. However, the genomic instability may also point to the cell radiosensitivity arising due to a dysfunction of DSB repair.

Consequently, we followed DSB repair kinetics and efficiency in NHDF fibroblasts and tumor cell primocultures after irradiation with a single dose of 2 Gy (1 Gy/min) of γ-rays. While the maximum average numbers of DSBs per nucleus induced by irradiation in $CD90^-$, $CD90^+$, and $CD90^-$ + $CD90^+$ primocultures varied with tumors, DSB repair kinetics was quite similar to (or even faster than in) NHDF fibroblasts for the radioresistant tumor analyzed (see Fig. 3).

On the other hand, the primocultures derived from the radiosensitive tumors (T1 and T3, Tab. 1) showed, relative to NHDF, significantly delayed DSB repair with a substantial fraction of DSBs persisting in cells for a long period of time (48 h) after irradiation. Hence, though general validity of described results and their connection to tumors' radioresistance at molecular level remain to be determined, it seems that radiosensitive tumors may exhibit defects or deregulation of DSB repair and at the same time do not tolerate persistent DSBs. On the other hand, it seems that radioresistant tumors can tolerate unrepaired DSBs and benefit from them. Unrepaired DSBs may increase genetic "dynamics" of radioresistant tumors and their adaptability (not only) to radiation-induced stress.

The defects in repair processes might be of epigenetic origin since otherwise the same genetic mutations would appear both in $CD90^-$ and $CD90^+$ cells of the tumor. However, even the "mutation" alternative does not seem to be unprecedented. For instance, in colon cancer, we revealed genetic changes even in cells of histologically normal tissue taken 10 cm far from the tumor [30].

Finally, $CD90^-$ and $CD90^+$ primocultures did not show striking differences in DSB repair characteristics.

However, for several tumors, lower numbers of γH2AX/53BP1 repair foci appeared upon irradiation in mixed $CD90^-$ + $CD90^+$ co-cultures than in $CD90^-$ or $CD90^+$ cells cultured separately (see Fig. 4); and existing foci also disappeared sooner from the former cells. In accordance with these results, we revealed that expression of some important genes in $CD90^+$ primocultures resembles more the situation in $CD90^-$ cells than in $CD90^+$ cells taken from histologically normal HN tissue. More efficient repair in $CD90^-$ + $CD90^+$ co-cultures may point to interactions between $CD90^-$ and $CD90^+$ cells that stimulate DSB repair.

5 Conclusions

In this work, we described our first results on DSB repair kinetics and efficiency in $CD90^-$ and $CD90^+$ cell primocultures isolated from radiosensitive and radioresistant HNSCC tumors, respectively. We demonstrated our ability to prepare $CD90^-$ and $CD90^+$ primocultures and follow DSB repair in these cells in vitro with highest possible sensitivity and precision. While the only radioresistant tumor in our study showed characteristics of DSB repair similar to normal human skin fibroblasts, both radiosensitive tumors exerted genetic instability and markedly delayed repair kinetics and increased persistence of unrepaired DSBs. Nevertheless, whether these results are more generally valid and monitoring of DSB repair can be used to predict the response of individual tumors to radiotherapy must be further studied.

This work was supported by the Czech Science Foundation (16-12454S).

Author contribution statement

Martin Falk and Michal Masarik designed the project, supervised the experiments and analyzed/interpreted the data. M.F. prepared the manuscript; Zuzana Horakova and Hana Binkova were responsible for clinical part of all works (patients diagnostics and follow up, tumors biopsies); Z.H. prepared clinical part of the manuscript; Jaromir Gumulec, Marketa Svobodova and Martina Raudenska isolated cells from patients tumors and prepared $CD90^-$ and $CD90^+$ cell primocultures; they also basically characterized gene expression of the primocultures; Olga Kopecna, Iva Falkova and Alena Bacikova participated in cell culturing, irradiated cells, and performed all immunofluorescence experiments on detection of γH2AX/53BP1 repair foci; O.K. also contributed to image analyses; Daniel Depes acquired microscopy images of γH2AX/53BP1 repair foci and analyzed the image data.

References

1. H. Binková, Otorinologie a foniatrie **59**, 114 (2010)
2. Z. Horáková, Otorinologie a foniatrie **59**, 107 (2010)
3. I. Falkova, Zdravotníctvo a Sociálna práca **11**, 19 (2016)
4. F. Perri, Head Neck **37**, 763 (2015)
5. G. Mountzios, Ann. Oncol. **25**, 1889 (2014)
6. W. Han, in *Advances in Genetics Research*, edited by K.V. Urbano (Nova Science, 2010)
7. T. Ettl, Oral Oncol. **51**, 158 (2015)
8. G. Peng, Mol. Med. Rep. **10**, 1709 (2014)
9. M. Maalouf, Int. J. Radiat. Oncol. Biol. Phys. **74**, 200 (2009)
10. Q. Wang, Int. J. Cancer **128**, 1546 (2011)
11. T. Kuilman, Genes Dev. **24**, 2463 (2010)
12. A. Lujambio, Bioessays **38**, S56 (2016)
13. L. Ježková, Appl. Radiat. Isot. **83(Pt B)**, 128 (2014)
14. M. Falk, Crit. Rev. Eukaryot. Gene Expr. **24**, 225 (2014)
15. J. Sevcik, Cell Signal. **24**, 1023 (2012)
16. J. Sevcik, Cell Signal. **25**, 1186 (2013)
17. A. Affolter, Oncol. Rep. **29**, 785 (2013)
18. X. Ji, Int. J. Clin. Exp. Med. **8**, 7002 (2015)
19. V. Salvatore, Oncotarget 1 (2016)
20. M. Falk, Appl. Radiat. Isot. **83**, 177 (2014)
21. M. Falk, Biochim. Biophys. Acta **1773**, 1534 (2007)
22. M. Kozubek, Cytometry **45**, 1 (2001)
23. P. Matula, in IEEE International Symposium on Biomedical Imaging: from Nano to Macro 2009 ISBI 09 (2009), p. 1138
24. M. Svobodova, Oncotarget, 2017, https://doi.org/10.18632/oncotarget.19914
25. B. Joshua, Head Neck **34**, 42 (2012)
26. M. Falk, Mutat. Res. **704**, 88 (2010)
27. M. Hofer, J. Med. Chem. **59**, 3003 (2016)
28. G. Wolf, Ear Nose Throat J. **80**, 897 (2001)
29. M. Raudenska, Tumour Biol. **36**, 9929 (2015)
30. E. Lukásová, Chromosoma **112**, 221 (2004)
31. E. Lukášová, Biochim. Biophys. Acta **1833**, 767 (2013)